ACS APPLIED MATERIALS & INTERFACES

Research Article

www.acsami.org

Metal–Organic Frameworks Modulated by Doping Er^{3+} for Up-Conversion Luminescence

Xindan Zhang,[†,‡] Bin Li,[*,†] Heping Ma,[*,†] Liming Zhang,[†] and Haifeng Zhao[†]

[†]State Key Laboratory of Luminescence and Applications, Changchun Institute of Optics Fine Mechanics and Physics, Chinese Academy of Sciences, Changchun 130033, P. R. China

[‡]University of Chinese Academy of Sciences, Beijing 100049, PR China

Supporting Information

ABSTRACT: Here we present metal–organic frameworks prepared by a one-step synthesis method, possessing both architectural properties of MOF building and up-conversion luminescence of rare earth Er^{3+} (hereafter denoted as Up-MOFs). Up-MOFs have characteristic up-conversion emissions at 520, 540, and 651 nm under the excitation of 980 nm owing to the multiple photon absorption. The up-conversion mechanism of these Up-MOFs has been discussed, and it can be attributed to the excited state absorption process. The design and synthesis of Up-MOF materials possessing near-infrared region excitation and up-conversion luminescence are fully expected to be candidates for the advancement of applications in bioimaging, sensors, optoelectronics, and energy conversion/storage devices.

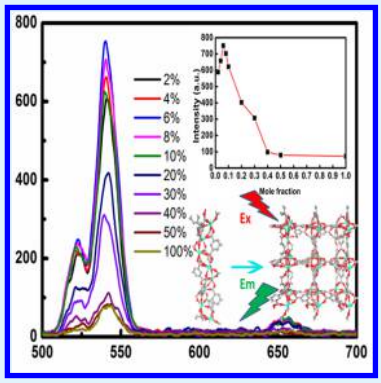

KEYWORDS: *up-conversion materials, metal–organic frameworks, near-infrared excitation, rare earth metal, excited state absorption (ESA)*

INTRODUCTION

In the past decade, up-conversion materials which have excitation at the near-infrared region (NIR) and emission at the visible region via a sequential absorption process of multiple photons have drawn wide attention among a growing body of researchers.[1−3] Benefitting from both the promising feature of being excited by NIR which is generally deemed as the "optical window in biological tissue" due to its reinforced light penetration depth and minimized autofluorescent interference[4] and intrinsic luminescent advantages such as sharp emission lines, long lifetimes, and superior photostability,[5] up-conversion materials are extremely suitable for the applications in biological imaging, photovoltaics, and photodynamical therapeutics.[6−9] Thus, there have been extensive investigations aiming at fabrication and exploitation of up-conversion materials. Among these studies, most up-conversion material syntheses are usually focused on nanocrystals which are composed of oxides (Y_2O_3, ZnO, $Yb_3Al_5O_{12}$, and so on) or fluorides (CaF_2, $NaYF_4$, $KMnF_3$, and so on) acting as an inorganic host matrix and embedded lanthanide ions (such as Er^{3+}, Tm^{3+}, Ho^{3+}) acting as luminescence centers. Therefore, exploiting new up-conversion systems such as inorganic–organic composite systems may achieve property synergies of inorganic rare earth ion and organic functional group targeting multiapplications.

Modern medical assay technologies mentioned above, where near-infrared excitation plays a vital part, are usually based on the photoluminescence method.[10−12] The traditional carriers for sensors or drugs, such as SiO_2 and MOFs, always need to offer extra space for luminescent materials which commonly provide the optical signal and then act as the markers after being excited, resulting in relatively poor luminescence efficiency and the bulky size of the assay system. In response to improve such medical applications, a novel porous material with intrinsic luminescence arouses our great interest.

Metal organic frameworks (MOFs) are emerging porous materials with hybrid inorganic–organic structure which comes from an assembly of metal clusters and organic building blocks.[13−15] Benefitting from the well-organized porosity and versatile chemical functionality, MOFs are of tremendous attractiveness and have great value in many fields such as gas storage and separation,[16−18] catalysis,[19] smart sensors,[20−23] and drug delivery.[24,25] As a unique type of MOFs, the lanthanide MOFs (Ln-MOFs) have drawn extensive attention due to their excellent luminescent character coming from doped lanthanide. Their intrinsic features of lanthanides together with the advantages of MOF structure provide eminent expectation for developing novel luminescent materials. By rational choices of rare earth ion and organic ligands, the synthesis process of Ln-MOFs has much flexibility of being elaborately controlled and tailored for featured luminescence properties.[26] Recently, several luminescent MOFs have been put forward by introducing various luminescent rare earth ions into basic

Received: March 30, 2016
Accepted: June 17, 2016
Published: June 17, 2016

DOI: 10.1021/acsami.6b03841
ACS Appl. Mater. Interfaces 2016, 8, 17389−17394

frameworks, and these MOFs have been widely used as fluorescence chemical sensors. However, the excitation wavelengths of these MOFs are mostly located at the ultraviolet region, in which situation the disadvantages of weak penetrability and autofluorescence interference from tissues and organs still exist and limit their applications in biology to a large extent. Undoubtedly, the fabrication of MOF materials possessing up-conversion luminescence which have excitation at the near-infrared region is becoming a promising candidate for the advancement of applications in bioimaging, sensors, optoelectronics, drug tracing, and energy conversion/storage devices.

Given the favorable structure of MOFs which could be modulated to finely optimize the photoluminescence performance of lanthanide ions, there is an ever-increasing interest in design and synthesis of porous MOF material with intrinsic up-conversion luminescence.[27,28] Here we report the study on a one-step strategy to prepare Er-doped Ln-MOFs with up-conversion luminescence (hereafter denoted as Up-MOFs) with uniform shape and tunable size. The Up-MOFs doped with Er^{3+} have characteristic up-conversion emissions at 520, 540, and 651 nm under the excitation at 980 nm owing to the multiple photon absorption process. Furthermore, the up-conversion mechanism of these Up-MOFs has been deeply discussed and attributed to excited state absorption (ESA). The fine-organized porosity and attractive luminescent properties of Up-MOF make it feasible for us to exploit the carrier suitable for detectable drug release or chemical sensing under near-infrared excitation. Furthermore, we also speculate the potential utility of such Up-MOF in energy and environment applications by virtue of its superior physical, chemical, and optical properties.

EXPERIMENTAL SECTION

Procedure for Synthesis of Standard Up-MOF. A homogeneous mixture of $ErCl_3{\cdot}6H_2O$ (0.006 mmol), $YCl_3{\cdot}6H_2O$ (0.094 mmol), H_3BTC (0.1 mmol), $NaAc{\cdot}3H_2O$ (0.1 mmol), *N*,*N*-dimethylformamide (8 mL), and deionized water (4 mL) was added into a sealed vial. Then the reaction vessel was heated at 60 °C for 1 day. The samples were washed with *N*,*N*-dimethylformamide several times. The above products were activated by being soaked in methanol lasting 1 day (each time using 50 mL of methanol and fresh methanol every 6 h). The final products were separated by filtering and dried under vacuum at 80 °C for 12 h.

Procedure for Synthesis of Other Types of Up-MOF. Y^{3+} could be replaced by other rare earth ions such as Yb^{3+}, Gd^{3+}, or Lu^{3+}. Given the same coordination numbers and modes, the concentration ratio between Er^{3+} and other diluent RE^{3+} could be adjusted by need on the premise that the total RE^{3+} was 0.1 mmol. White crystalline powder was obtained following the identical means of preparation of standard Up-MOF mentioned previously.

RESULTS AND DISCUSSION

Morphology and Structure of Up-MOFs. Different from the conventional postsynthetic modification (PSM)[29] of MOFs in which situation chemical modifications are performed after the preparation of MOFs, Up-MOFs of $RE(BTC)(H_2O){\cdot}DMF$, where RE could be Er^{3+}, Y^{3+}, Lu^{3+}, Gd^{3+}, or Yb^{3+} and BTC = 1,3,5-benzenetricarboxylic acid, were one-step synthesized through a solvothermal method similar to the study reported previously.[30] Sodium acetate is selected as a capping reagent in order to modulate crystal morphology and size. The resultant Up-MOF is a 3D porous framework crystallized in the $P4_322$ space group. Every building unit includes one rare earth ion (such as Er^{3+}, Y^{3+}) with seven coordination sites, bonding with one BTC ligand and one coordinated water molecule. As depicted in Scheme 1(a), the special connection mode of rare earth ions results in a one-dimensional helical chain along the [001] direction, and then, inorganic chains in one dimension connected by phenyl groups along [100] and [010] directions give rise to a framework in three dimensions (as depicted in Scheme 1(b)).[31]

Scheme 1. (a) 1D Chains Views in Up-MOFs along [001] the Direction and (b) 3D Structure Images of (001) Faces in Up-MOFs with 1D Channels[a]

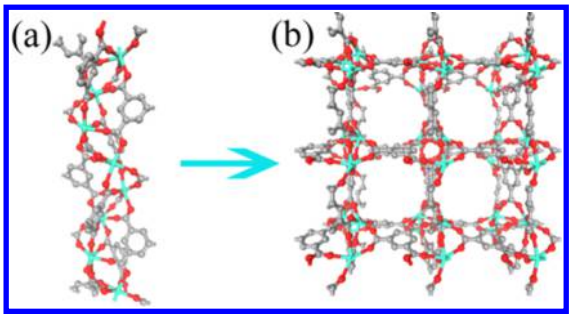

[a]C atom: gray; O atom: red; rare earth ions: bright blue; H atoms are omitted for clarity.

The structures of the as-synthesized samples are demonstrated by powder XRD pattern and presented in Figure 1. The PXRD patterns which are well conformed to previous literature suggest that Up-MOFs are isostructural and well-indexed to the known bulk phase of JUC-32.[32] As depicted in Figure 1, PXRD patterns of Up-MOF-Y/Er (black line, d) and other Up-MOFs doped with different rare earth ions at the same concentration ratio of rare earth to H_3BTC are almost identical, indicating the unchanged crystal structure after ion replacement because of the same coordination numbers and modes of diverse rare earth ions of Er^{3+}, Y^{3+}, Gd^{3+}, Lu^{3+}, or Yb^{3+}. The slight shift of diffraction peaks of Up-MOFs in our case can be explained by the lanthanide contraction.[15]

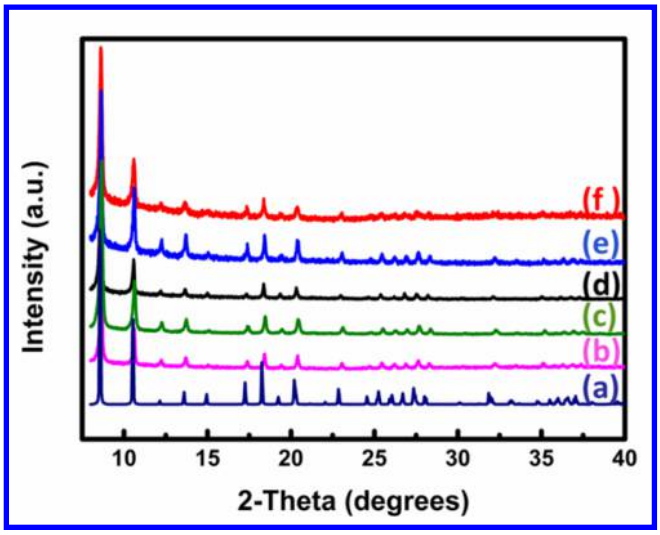

Figure 1. PXRD patterns of Up-MOFs (a) simulated, (b) doped with Gd/Er, (c) doped with Lu/Er, (d) doped with Y/Er, (e) doped with Yb/Er, and (f) totally doped with Er.

DOI: 10.1021/acsami.6b03841
ACS Appl. Mater. Interfaces 2016, 8, 17389−17394

The morphologies of the standard Up-MOF are monitored by scanning electron microscopy. The SEM images (Figure 2)

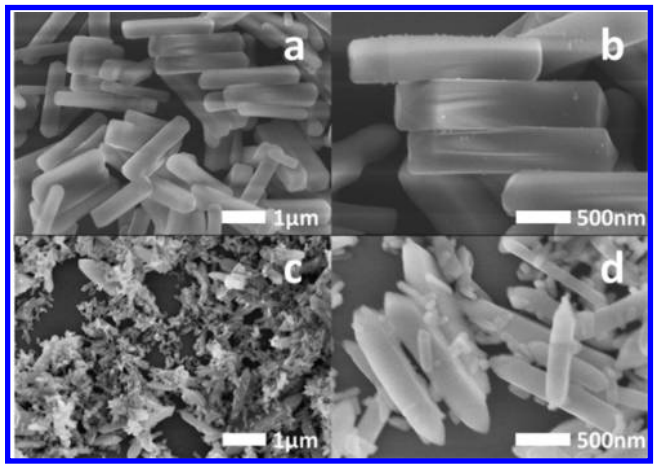

Figure 2. SEM images of standard Up-MOF crystals synthesized with (a),(b) and without (c),(d) addition of sodium acetate at different magnifications. Scale bars: 1 μm (a, c), 500 nm (b, d).

exhibit that rod-like standard Up-MOFs are highly uniform crystals with the width of 0.4 μm and the length of 2 μm. Here, sodium acetate acting as a capping reagent in the process of MOF formation besides BTC provides positive effects on the crystal quality and size. The influence of sodium acetate on controlling the MOF size and then generating relatively uniform morphology comes from its improvements in coordinating interactions between the rare earth ions and organic ligands. In the preliminary stage of crystal formation, the RE^{3+} bonds with the carboxylic groups from both the organic linker of BTC and sodium acetate added. Therefore, the crystal growth is hindered in this period, resulting in more nuclei processes. Moreover, the competitive bonding between capping reagents and BTC is speculated to regulate the rate of MOF formation.[33] When no sodium acetate was added, we observe the rod-like crystals with nonuniform phase from SEM images (Figure 2c and 2d). Furthermore, the elemental analysis characterization of Up-MOF-Y/Er is investigated by EDX. As shown in Figure S1, representative peaks associated with Y, Er, C, and O elements which consist of standard Up-MOF together are clearly identified.

The permanent porosity of Up-MOFs-Y/Er is demonstrated by measuring N_2 adsorption at 77 K. Before the measurement, the samples were treated with degassing at 200 °C overnight. As depicted in Figure S2, Up-MOFs display a typical characteristic of microporous materials which has been widely used as a drug carrier.[31,34] The calculated BET surface area is 59.28 m^2/g, and the Langmuir surface area is 72.87 m^2/g. In order to investigate the feasibility of Up-MOF in drug release, we design primary measurement of drug release by using ibuprofen (IBU), which has been widely utilized as a model drug in research of drug delivery and tracing. We monitor the absorption spectra of supernatant after the IBU-loaded Up-MOFs were placed into PBS solution which is widely used for diluting biologicals. The absorption spectra and corresponding profiles versus release time are shown in Figure S3, exhibiting the capability of Up-MOFs in sustained drug release. These results demonstrate that such an Up-MOF system which benefits from up-conversion characteristic and MOF structure is promising as a candidate of the carrier used for detectable drug release. Next, we desire to fully examine the biocompatibility of such Up-MOFs for the further biological applications.

Photoluminescence Properties of Up-MOFs. In our case, the Y^{3+} ion which lacks ^{4}f orbitals is relatively inert to be a luminescent center; therefore, it just acts as the ion diluent and has negligible interaction with emitting dopant of Er^{3+}. The up-conversion luminescence (UCL) spectra of the Up-MOF-$Y_{1-\chi}$/Er_χ (χ is the mole fraction of Er^{3+} in total RE^{3+}) are tested under the 980 nm excitation. As shown in Figure 3, Up-MOF-

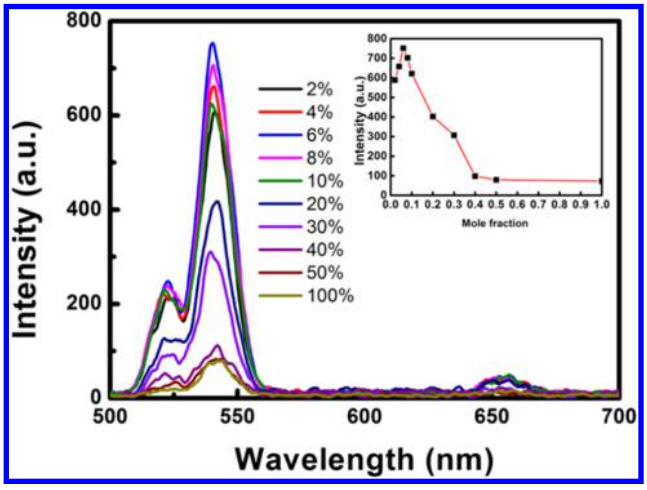

Figure 3. UCL of Up-MOF-$Y_{1-\chi}$/Er_χ with different concentration of Er^{3+} (range of χ is from 2% to 100%) with the excitation at 980 nm.

Y/Er with different Er^{3+} concentration all exhibit characteristic emissions at 520, 540, and 651 nm, respectively, ascribed to the allowed electronic transition from $^2H_{11/2}$ to $^4I_{15/2}$, from $^4S_{3/2}$ to $^4I_{15/2}$, and from $^4F_{9/2}$ to $^4I_{15/2}$.[35] Along with increasing concentrations of Er^{3+} ions from 2% to 100% in mole fraction, the UCL intensity especially at 540 nm elevates at low Er^{3+} concentration and reaches maxima at 6% Er^{3+} content, corresponding to the maximum of quantum yield of 0.1312%. Due to the concentration quenching effect, the UCL intensity of Up-MOF-Y/Er drastically decreases when the Er^{3+} concentration is more than 10%. The optimal concentration of doped Er^{3+} ions is demonstrated to be 6%, beyond which the concentration quenching effect will dominate over the increase of activator centers. The concentration quenching originates from the larger probability of energy loss at a killer center due to excitation energy migration among activators of Er^{3+} at higher concentration.[36]

Photoluminescence Mechanism of Up-MOFs. Based on the understanding of traditional up-conversion materials with inorganic matrix such as $NaYF_4$:Yb^{3+}/Er^{3+}, the ion of Yb has always been selected as a sensitizer by providing the $^2F_{5/2}$ energy level in the energy transfer up-conversion (ETU) process.[37] We fabricated the Up-MOFs codoped with Y^{3+}, Yb^{3+}, and Er^{3+} (mole ratios of Y/Yb/Er are 60/30/10, 30/60/10, and 0/90/10, respectively) to investigate the effect of Yb^{3+}, where Y^{3+} just acts as a kind of ion diluent because of a lack of ^{4}f energy level. However, the spectra of Up-MOF-Y/Yb/Er with the distinctly different doping concentration of Yb^{3+} show the same emission intensity (Figure 4), indicating that the up-conversion mechanism of Up-MOFs is speculated to arise from excited state absorption of Er^{3+} by the interaction between multiple photons and metastable energy level rather than an

DOI: 10.1021/acsami.6b03841
ACS Appl. Mater. Interfaces 2016, 8, 17389−17394

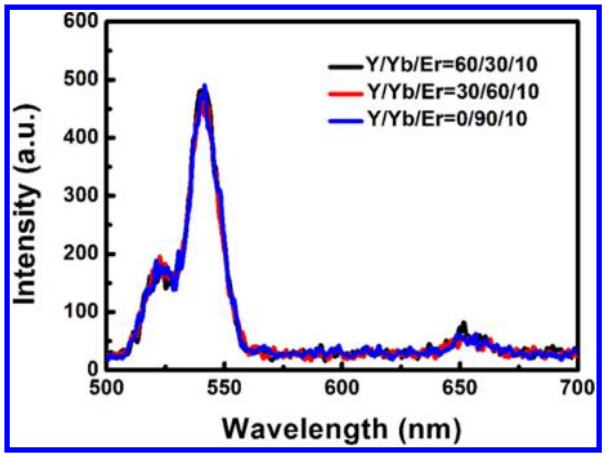

Figure 4. UCL of Up-MOFs codoped with Y, Yb, and Er in different molar ratio.

energy transfer up-conversion process like inorganic matrix up-conversion materials of $NaYF_4$:Yb^{3+}/Er^{3+}.[38]

To further investigate the UC mechanism of Up-MOFs-$Y_{0.94}/Er_{0.06}$ (standard, mole ratio of Y:Er is 94:6), the relationship between pumping power and luminescent intensity has been measured (shown in Figure 5). Typically, for an

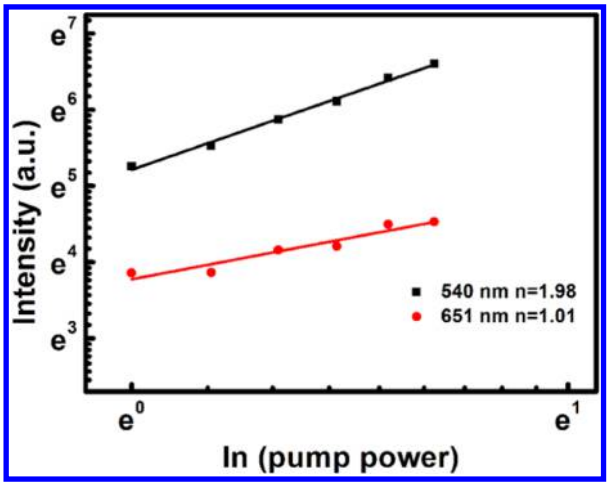

Figure 5. Plot (ln−ln) of up-conversion intensity versus excitation power (standard Up-MOFs-Y/Er).

unsaturated up-conversion process, the emission intensity is strongly dependent on its local environment and obeys an empirical relation that is given as[39,40]

$$I_f \propto P^n \quad (1)$$

The relation demonstrates that the fluorescent intensity (I_f) is proportional to the nth power of the excitation (P); meanwhile, n represents the number denoting photons absorbed in per up-converted process (often take the first integer more than n when n is not an integer). Figure 5 indicates the dependence of UC intensity on the laser power: calculated n = 1.98 and 1.01 for 540 and 651 nm emissions, respectively. These facts mean that populations on states of $^4S_{3/2}$ and $^4F_{9/2}$ result from two-photon UC processes at least. Due to the existence of the cross-relaxation and nonradiative transitions in MOFs, we can deduce that the UC process results from the multiphoton absorption process of Er^{3+}, and the exact number of photons is far more than 2.

To further understand the up-conversion mechanism of Up-MOFs, we measure the absorption spectra of various samples, and the results are shown in Figure S4. The absorption spectra of various Up-MOFs exhibit a relatively wide absorption band from ∼960 to ∼1150 nm which should be caused by an organic matrix and may further lead to ligand-to-metal energy transition.[41,42] This observation also demonstrates the existence of coordination bonds between Er^{3+} and carboxyl from organic ligands.

Based on the above analysis, the UC emission of Up-MOF-Y/Er has been further demonstrated to be the excited state absorption process in trivalent Er ions. A scheme of up-conversion energy transfer process in Er^{3+}-based MOF is exhibited in Figure 6. Absorption at 980 nm is followed by

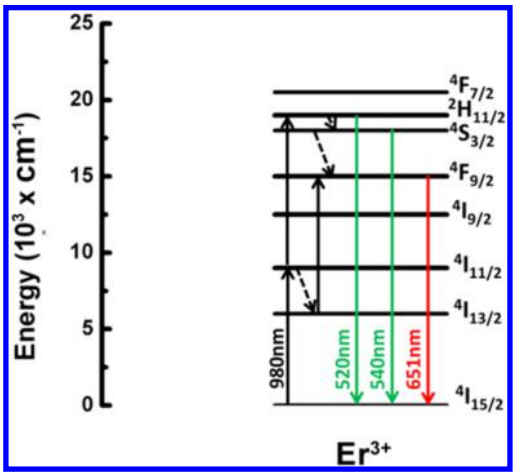

Figure 6. Up-conversion energy scheme of Er^{3+} from near-infrared excitation to visible emission.

energy transfer to the $^4I_{11/2}$ energy level of Er^{3+}. Subsequently, the second absorption leads to the population at a higher energy level of $^2H_{11/2}$. By virtue of the nonradiative relaxation processes ($^2H_{11/2} \rightarrow {}^4S_{3/2}$), absorbed photons lead to two primary emissions at 520 nm (from $^2H_{11/2}$ to $^4I_{15/2}$) and 540 nm (from $^4S_{3/2}$ to $^4I_{15/2}$) which locate in the green-light region via radiative transition. Also, two near-infrared photons may be absorbed sequentially by one Er^{3+} and used to promote electronic population to high-lying energy levels, and such excited state population finally emits red light of 651 nm via the relaxation back to the ground state through the transition of $^2H_{11/2} \rightarrow {}^4S_{3/2} \rightarrow {}^4F_{9/2} \rightarrow {}^4I_{15/2}$. It is possible that other excitation routes for level $^4F_{9/2}$ derived from the interactions of neighboring Er^{3+} exist.[38] However, detailed investigation of such a process is beyond the scope of the current work, and it can be explained by a previously published study.[43]

To further demonstrate the up-conversion process, the UCL lifetime of the standard Up-MOFs-Y/Er at 540 nm under pulse laser excitation of 980 nm has also been measured and plotted in Figure 7. Obviously, the entire lifetime consists of a population curve and decay curve, suggesting that the emission results from an up-conversion process. The decay curve is well conformed to a single exponential function with the decay time of 133.89 μs, which is consistent with the decay time of Er^{3+} in other up-conversion materials.[44] Generally, up-conversion materials suffer from the situation of low quantum efficiency because of the existing of a mount of nonradiative relaxation process and the susceptibility to complex dispersion environ-

DOI: 10.1021/acsami.6b03841
ACS Appl. Mater. Interfaces 2016, 8, 17389−17394

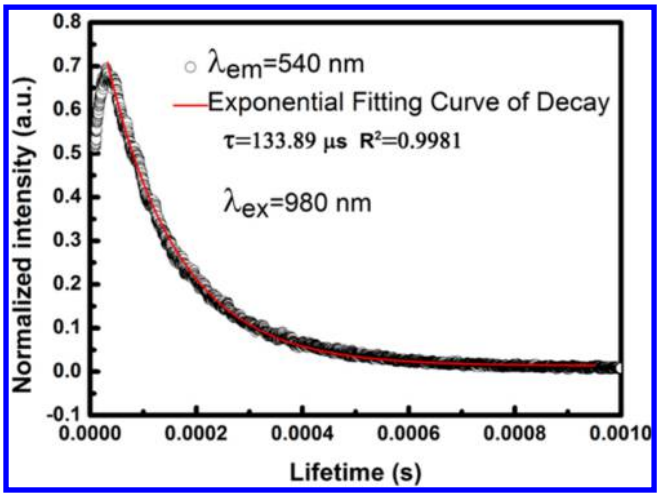

Figure 7. Time evolution and single exponential fitting curve of the green UCL (540 nm) of standard Up-MOF-Y/Er under pulse laser excitation at 980 nm.

ment. Hence, we will particularly focus on enhancing up-conversion emission intensity in the further study.

CONCLUSIONS

In summary, a series of metal−organic frameworks with up-conversion luminescence under NIR excitation have been successfully fabricated via a facile and simple one-step synthesis method. After being comprehensively characterized by a suite of measurements such as SEM, PXRD, PL, and so on, it is demonstrated that Up-MOFs fully display the merits of structure stability, porosity nature, and valuable up-conversion characteristic under near-infrared light excitation of 980 nm. Moreover, the up-conversion mechanisms have been deeply investigated and attributed to ESA. The fine-organized porosity and multifunctionality of Up-MOF offer the possibility for us to develop an attractive carrier which is extremely suitable for biological applications in drug release or chemical sensing with the help of a detectable optical signal under near-infrared excitation. Basic drug release performance has been examined and proves the feasibility. This work also broadens the scope of potential energy and environment applications such as in optoelectronics, catalysis, and energy conversion/storage devices owing to its superior physical, chemical, and optical properties.

ASSOCIATED CONTENT

Supporting Information

The Supporting Information is available free of charge on the ACS Publications website at DOI: 10.1021/acsami.6b03841.

Chemicals and materials. Characterization. Elemental analysis characterization of Up-MOF-Y/Er. N_2 adsorption and desorption isotherm of Up-MOFs measured at 77 K. Drug release performance in the system of IBU-loaded Up-MOFs. UV−vis absorption spectra of different Up-MOFs dispersed in H_2O solution (PDF)

AUTHOR INFORMATION

Corresponding Authors

*E-mail: libinteacher@163.com (B. Li).
*E-mail: mahp@ciomp.ac.cn (H. Ma).

Notes

The authors declare no competing financial interest.

ACKNOWLEDGMENTS

The authors greatly thank the financial support of the NSFC (Grant Nos. 51372240, 51572256, 21501166).

REFERENCES

(1) Wu, D. M.; Garcia-Etxarri, A.; Salleo, A.; Dionne, J. A. Plasmon-Enhanced Upconversion. *J. Phys. Chem. Lett.* **2014**, *5*, 4020−4031.
(2) Chen, G.; Qju, H.; Prasad, P. N.; Chen, X. Upconversion Nanoparticles: Design, Nanochemistry, and Applications in Theranostics. *Chem. Rev.* **2014**, *114*, 5161−5214.
(3) Pattelli, L.; Savo, R.; Burresi, M.; Wiersma, D. S. Spatio-temporal Visualization of Light Transport in Complex Photonic Structures. *Light: Sci. Appl.* **2016**, *5*, e16090.
(4) Park, W.; Lu, D.; Ahn, S. Plasmon Enhancement of Luminescence Upconversion. *Chem. Soc. Rev.* **2015**, *44*, 2940−2962.
(5) Ding, Y.; Zhu, H.; Zhang, X.; Gao, J.; Abdel-Halim, E. S.; Jiang, L.; Zhu, J. J. An Upconversion Nanocomposite for Fluorescence Resonance Energy Transfer Based Cholesterol-sensing in Human Serum. *Nanoscale* **2014**, *6*, 14792−14798.
(6) Sun, L. N.; Peng, H.; Stich, M. I.; Achatz, D.; Wolfbeis, O. S. pH Sensor Based on Upconverting Luminescent Lanthanide Nanorods. *Chem. Commun.* **2009**, 5000−5002.
(7) Yuan, P.; Lee, Y. H.; Gnanasammandhan, M. K.; Guan, Z.; Zhang, Y.; Xu, Q. H. Plasmon Enhanced Upconversion Luminescence of $NaYF_4$:Yb,Er@SiO_2@Ag Core-shell Nanocomposites for Cell Imaging. *Nanoscale* **2012**, *4*, 5132−5137.
(8) Xu, S.; Xu, S.; Zhu, Y.; Xu, W.; Zhou, P.; Zhou, C.; Dong, B.; Song, H. A Novel Upconversion, Fluorescence Resonance Energy Transfer Biosensor (FRET) for Sensitive Detection of Lead Ions in Human Serum. *Nanoscale* **2014**, *6*, 12573−12579.
(9) Wang, J.; Deng, R.; MacDonald, M. A.; Chen, B.; Yuan, J.; Wang, F.; Chi, D.; Hor, T. S.; Zhang, P.; Liu, G.; Han, Y.; Liu, X. Enhancing Multiphoton Upconversion through Energy Clustering at Sublattice Level. *Nat. Mater.* **2014**, *13*, 157−162.
(10) Ai, K.; Zhang, B.; Lu, L. Europium-based Fluorescence Nanoparticle Sensor for Rapid and Ultrasensitive Detection of an Anthrax Biomarker. *Angew. Chem., Int. Ed.* **2009**, *48*, 304−308.
(11) Li, C.; Liu, J.; Alonso, S.; Li, F.; Zhang, Y. Upconversion Nanoparticles for Sensitive and In-depth Detection of Cu^{2+} Ions. *Nanoscale* **2012**, *4*, 6065−6071.
(12) Liu, J.; Li, C.; Li, F. Fluorescence Turn-on Chemodosimeter-functionalized Mesoporous Silica Nanoparticles and Their Application in Cell Imaging. *J. Mater. Chem.* **2011**, *21*, 7175−7181.
(13) Yaghi, O. M.; O'Keeffe, M.; Ockwig, N. W.; Chae, H. K.; Eddaoudi, M.; Kim, J. Reticular Synthesis and the Design of New Materials. *Nature* **2003**, *423*, 705−714.
(14) Lu, G.; Li, S.; Guo, Z.; Farha, O. K.; Hauser, B. G.; Qi, X.; Wang, Y.; Wang, X.; Han, S.; Liu, X.; DuChene, J. S.; Zhang, H.; Zhang, Q.; Chen, X.; Ma, J.; Loo, S. C.; Wei, W. D.; Yang, Y.; Hupp, J. T.; Huo, F. Imparting Functionality to a Metal-organic Framework Material by Controlled Nanoparticle Encapsulation. *Nat. Chem.* **2012**, *4*, 310−316.
(15) Ferey, G. Hybrid Porous Solids: Past, Present, Future. *Chem. Soc. Rev.* **2008**, *37*, 191−214.
(16) Demessence, A.; Boissière, C.; Grosso, D.; Horcajada, P.; Serre, C.; Férey, G.; Soler-Illia, G. J. A. A.; Sanchez, C. Adsorption Properties in High Optical Quality Nano ZIF-8 Thin Films with Tunable Thickness. *J. Mater. Chem.* **2010**, *20*, 7676−7681.
(17) Liu, X.; He, L.; Zheng, J.; Guo, J.; Bi, F.; Ma, X.; Zhao, K.; Liu, Y.; Song, R.; Tang, Z. Solar-Light-Driven Renewable Butanol Separation by Core-Shell Ag@ZIF-8 Nanowires. *Adv. Mater.* **2015**, *27*, 3273−3277.
(18) Zhao, X.; Xiao, B.; Fletcher, A. J.; Thomas, K. M.; Bradshaw, D.; Rosseinsky, M. J. Hysteretic Adsorption and Desorption of Hydrogen

DOI: 10.1021/acsami.6b03841
ACS Appl. Mater. Interfaces 2016, 8, 17389−17394

by Nanoporous Metal-Organic Frameworks. *Science* **2004**, *306*, 1012−1015.
(19) Park, K. H.; Jang, K.; Son, S. U.; Sweigart, D. A. Self-Supported Organometallic Rhodium Quinonoid Nanocatalysts for Stereoselective Polymerization of Phenylacetylene. *J. Am. Chem. Soc.* **2006**, *128*, 8740−8741.
(20) Chen, B.; Wang, L.; Zapata, F.; Qian, G.; Lobkovsky, E. B. A Luminescent Microporous Metal−Organic Framework for the Recognition and Sensing of Anions. *J. Am. Chem. Soc.* **2008**, *130*, 6718−6719.
(21) Kreno, L. E.; Hupp, J. T.; Duyne, R. P. V. Metal-Organic Framework Thin Film for Enhanced Localized Surface Plasmon Resonance Gas Sensing. *Anal. Chem.* **2010**, *82*, 8042−8046.
(22) He, L.; Liu, Y.; Liu, J.; Xiong, Y.; Zheng, J.; Liu, Y.; Tang, Z. Core-shell Noble-metal@metal-organic-framework Nanoparticles with Highly Selective Sensing Property. *Angew. Chem., Int. Ed.* **2013**, *52*, 3741−3745.
(23) Han, S.; Warren, S. C.; Yoon, S. M.; Malliakas, C. D.; Hou, X.; Wei, Y.; Kanatzidis, M. G.; Grzybowski, B. A. Tunneling Electrical Connection to the Interior of Metal-Organic Frameworks. *J. Am. Chem. Soc.* **2015**, *137*, 8169−8175.
(24) Vallet-Regi, M.; Balas, F.; Arcos, D. Mesoporous Materials for Drug Delivery. *Angew. Chem., Int. Ed.* **2007**, *46*, 7548−7558.
(25) Horcajada, P.; Chalati, T.; Serre, C.; Gillet, B.; Sebrie, C.; Baati, T.; Eubank, J. F.; Heurtaux, D.; Clayette, P.; Kreuz, C.; Chang, J. S.; Hwang, Y. K.; Marsaud, V.; Bories, P. N.; Cynober, L.; Gil, S.; Ferey, G.; Couvreur, P.; Gref, R. Porous Metal-organic-framework Nanoscale Carriers as a Potential Platform for Drug Delivery and Imaging. *Nat. Mater.* **2010**, *9*, 172−178.
(26) Zhang, S. Y.; Shi, W.; Cheng, P.; Zaworotko, M. J. A Mixed-Crystal Lanthanide Zeolite-like Metal-Organic Framework as a Fluorescent Indicator for Lysophosphatidic Acid, a Cancer Biomarker. *J. Am. Chem. Soc.* **2015**, *137*, 12203−12206.
(27) Yang, J.; Yue, Q.; Li, G.-D.; Cao, J.-J.; Li, G.-H.; Chen, J. S. Structures, Photoluminescence, Up-Conversion, and Magnetism of 2D and 3D Rare-Earth Coordination Polymers with Multicarboxylate Linkages. *Inorg. Chem.* **2006**, *45*, 2857−2865.
(28) Mahata, P.; Ramya, K. V.; Natarajan, S. Pillaring of $CdCl_2$-like Layers in Lanthanide Metal-organic Frameworks: Synthesis, Structure, and Photophysical Properties. *Chem. - Eur. J.* **2008**, *14*, 5839−5850.
(29) An, J.; Shade, C. M.; Chengelis-Czegan, D. A.; Petoud, S.; Rosi, N. L. Zinc-Adeninate Metal−Organic Framework for Aqueous Encapsulation and Sensitization of Near-infrared and Visible Emitting Lanthanide Cations. *J. Am. Chem. Soc.* **2011**, *133*, 1220−1223.
(30) Qian, J. J.; Qiu, L. G.; Wang, Y. M.; Yuan, Y. P.; Xie, A. J.; Shen, Y. H. Fabrication of Magnetically Separable Fluorescent Terbium-based MOF Nanospheres for Highly Selective Trace-level Detection of TNT. *Dalton Trans.* **2014**, *43*, 3978−3983.
(31) Guo, X.; Zhu, G.; Li, Z.; Sun, F.; Yang, Z.; Qiu, S. A Lanthanide Metal-organic Framework with High Thermal Stability and Available Lewis-acid Metal Sites. *Chem. Commun.* **2006**, 3172−3174.
(32) Li, Z.; Zhu, G.; Lu, G.; Qiu, S.; Yao, X. Ammonia Borane Confined by a Metal−Organic Framework for Chemical Hydrogen Storage: Enhancing Kinetics and Eliminating Ammonia. *J. Am. Chem. Soc.* **2010**, *132*, 1490−1491.
(33) Guo, H.; Zhu, Y.; Qiu, S.; Lercher, J. A.; Zhang, H. Coordination Modulation Induced Synthesis of Nanoscale $Eu_{(1-x)}Tb_{(x)}$-metal-organic Frameworks for Luminescent Thin Films. *Adv. Mater.* **2010**, *22*, 4190−4192.
(34) Ma, H.; Ren, H.; Meng, S.; Yan, Z.; Zhao, H.; Sun, F.; Zhu, G. A 3D Microporous Covalent Organic Framework with Exceedingly High C_3H_8/CH_4 and C_2 Hydrocarbon/CH_4 Selectivity. *Chem. Commun.* **2013**, *49*, 9773−9775.
(35) Zhang, J.; Hao, Z.; Li, J.; Zhang, X.; Luo, Y.; Pan, G. Observation of Efficient Population of the Red-emitting State from the Green State by Non-multiphonon Relaxation in the Er^{3+}−Yb^{3+} System. *Light: Sci. Appl.* **2015**, *4*, e239.
(36) Xiao, W.; Zhang, X.; Hao, Z.; Pan, G. H.; Luo, Y.; Zhang, L.; Zhang, J. Blue-emitting K2Al2B2O7:Eu(2+) Phosphor with High Thermal Stability and High Color Purity for Near-UV-pumped White Light-emitting Diodes. *Inorg. Chem.* **2015**, *54*, 3189−3195.
(37) Qin, W. P.; Liu, Z. Y.; Sin, C. N.; Wu, C. F.; Qin, G. S.; Chen, Z.; Zheng, K. Z. Multi-ion Cooperative Processes in Yb^{3+} Clusters. *Light: Sci. Appl.* **2014**, *3*, e193.
(38) Rakov, N.; Guimarães, R. B.; Franceschini, D. F.; Maciel, G. S. Er:SrF_2 Luminescent Powders Prepared by Combustion Synthesis. *Mater. Chem. Phys.* **2012**, *135*, 317−321.
(39) Wang, G.; Qin, W.; Zhang, J.; Zhang, J.; Wang, Y.; Cao, C.; Wang, L.; Wei, G.; Zhu, P.; Kim, R. Synthesis, Growth Mechanism, and Tunable Upconversion Luminescence of Yb^{3+}/Tm^{3+}-Codoped YF_3 Nanobundles. *J. Phys. Chem. C* **2008**, *112*, 12161−12167.
(40) Yu, D. C.; Martin-Rodriguez, R.; Zhang, Q. Y.; Meijerink, A.; Rabouw, F. T. Multi-photon Quantum Cutting in Gd_2O_2S:Tm^{3+} to Enhance the Photo-response of Solar Cells. *Light: Sci. Appl.* **2015**, *4*, e344.
(41) Hao, J. N.; Yan, B. Ag^+-sensitized Lanthanide Luminescence in Ln^{3+} Post-functionalized Metal-organic Frameworks and Ag^+ Sensing. *J. Mater. Chem. A* **2015**, *3*, 4788−4792.
(42) Hao, J. N.; Yan, B. Highly Sensitive and Selective Fluorescent Probe for Ag^+ Based on a Eu^{3+} Post-Functionalized Metal-organic Framework in Aqueous Media. *J. Mater. Chem. A* **2014**, *2*, 18018−18025.
(43) Rakov, N.; Guimaraes, R. B.; Maciel, G. S. Strong Infrared-to-visible Frequency Upconversion in Er^{3+}-doped Sr_2CeO_4 Powders. *J. Lumin.* **2011**, *131*, 342−346.
(44) Vetrone, F.; Naccache, R.; Mahalingam, V.; Morgan, C. G.; Capobianco, J. A. The Active-Core/Active-Shell Approach: A Strategy to Enhance the Upconversion Luminescence in Lanthanide-Doped Nanoparticles. *Adv. Funct. Mater.* **2009**, *19*, 2924−2929.

DOI: 10.1021/acsami.6b03841
ACS Appl. Mater. Interfaces 2016, 8, 17389−17394